[Summary of Doctoral Dissertation]

Synthesis and Femtosecond Laser Excited-Terahertz Wave Emission of Cu-based and ZnTe Nano/Micro Materials

CHAU Yuen Ting Rachel

[Background and Objectives]

This dissertation focuses on the syntheses and applications of Cu-based and ZnTe nano/micro materials. Bottom-up approaches (e.g., wet-chemical synthesis, thermal decomposition) are commonly used to prepare nano/micro materials. Although sizes and morphologies of nano/micro materials are easily controlled with bottom-up approaches, these approaches are not conducive for making alloy nanomaterials due to the difference in reduction potentials of different metals, which a heterostructure is formed easily instead of the solid-solution alloy.[1] Top-down approaches (e.g., thermal evaporation, sputter deposition) are used for making alloy nanomaterials by evaporating the bulk materials under vacuum. For example, the use of alloy targets yields alloy nanomaterials.[2] Compositional-tunable alloy nanomaterials could also be obtained by varying sputter currents to the targets in a co-sputtering system.[3-4] Considerations of choosing appropriate method to obtain desired nano/micro materials are discussed. Moreover, Cu-based (metal, alloys, oxides, heterostructures) and ZnTe materials give optical responses with respect to the excitation.[5-8] With the development of ultrafast laser pulse technologies in recent decades, materials are found to emit electromagnetic wave in terahertz regime when they are irradiated by femtosecond laser pulses.[9-10] Terahertz wave generation from the photocarriers acceleration from depletion field formed by metal/semiconductor interface (e.g., Cu_xO/Au)[11-14] and from non-centrosymmetric

single crystals (e.g., ZnTe [15] and GaAs [16]) via optical rectification have been concerned. This thesis aims at discussing the mechanism of terahertz wave emission from Cu-based oxides and their heterostructures, and the possibility of replacing conventional ZnTe single crystal by polycrystalline ZnTe microspheres as the terahertz wave source.

[Experimental methods]

In Chapter 2, monometallic Cu and bimetallic Cu-Pd nanoparticles dispersed in liquid polyethylene glycol (PEG) were synthesized using sputter deposition under 2 Pa of argon pressure. Single target sputtering was used to synthesize monometallic Cu nanoparticles. The sputtering current was 50 mA. Double target co-sputtering was performed to synthesize bimetallic Cu-Pd nanoparticles. 10, 30, 50 mA of sputtering current was applied to the metal target respectively to obtain Cu-Pd nanoparticles with different compositions. Sputtering time was 30 min. Characterizations (UV-vis, TEM, XPS, XRD, HAADF-STEM, EDS) were carried out to evaluate the optical properties, sizes and morphologies, and compositions of sputtered nanoparticles. The stabilities of dispersion stored in air were also monitored.

In Chapter 3, Au@Cu_2O heterostructure core-shell nanoparticles dispersion was synthesized using wet-chemical synthesis. Au@Cu_2O nanoparticles was formed by mixing Au nanoparticles, anhydrous copper (II) chloride ($CuCl_2$), sodium dodecyl sulfate (SDS), and hydroxylamine hydrochloride ($NH_2OH{\cdot}HCl$) in an alkaline solution. Different concentration of $CuCl_2$ were added during synthesis to obtain shell-thickness tunable Au@Cu_2O nanoparticles. The stability of Au@Cu_2O core-shell nanoparticles in mixed solvents of ethanol/water with different compositions was monitored to evaluate the suitability of using Au@Cu_2O heterostructure core-shell nanoparticles as terahertz wave

sources.

In Chapter 4, Cu single-layered and Cu/Au double-layered structures were fabricated on Si wafer using sputter deposition. Samples were oxidation annealed at different temperatures (80, 110, 140, 170, 200, 250, 300 ℃) for 2 h in air. XRD and TEM-SAED were used to identify the oxidation degrees of Cu layer and the location that Cu oxidization initiated. Samples were irradiated by femtosecond laser (35 fs, 800 nm, 1 kHz) pulses and terahertz radiation emitted from samples were detected using terahertz time-domain spectroscopy with an electrooptic sampling crystal.

In Chapter 5, ZnTe microspheres were synthesized in the ethylene glycol (EG) solution using a novel hot injection method. EG with different amount of poly(N-vinyl-2-pyrrolidone) (PVP) was heated to 200 ℃, followed with injection of zinc chloride ($ZnCl_2$) and sodium tellurite (Na_2TeO_3) contained precursor solution to obtain ZnTe microspheres with different sizes. The formation of ZnTe microspheres in 518 mg of PVP contained ethylene glycol was monitored from 0.2 to 48 h. Different sized ZnTe microspheres were deposited onto Si wafer and irradiated by femtosecond laser (35 fs, 800 nm, 1 kHz) pulses and terahertz radiation emitted from ZnTe microspheres were detected using terahertz time-domain spectroscopy with an electrooptic sampling crystal.

[Results and Discussion]

Chapter 2 presented both Cu and Cu-Pd nanoparticles had size less than 5 nm. All nanoparticles were well dispersed in PEG without aggregation. UV-vis spectrum of monometallic Cu nanoparticles dispersion showed an absorption peak at 570 nm, which was originated from Cu nanoparticles. The absorption characteristic faded out from day 2 after sputtering, indicating the Cu nanoparticles had been oxidized naturally in PEG

under air. Oxidation of Cu were also found in Cu-Pd alloy nanoparticles. Table 1 lists Pd content of Cu-Pd nanoparticles determined by XRD, XPS, mass measurement and STEM-EDS with respect to sputtering current combinations for Cu and Pd metal targets. All measurements were conducted with freshly prepared samples except STEM-EDS. It is suspected that Cu atoms oxidized and dissolved into PEG during storage, therefore the STEM-EDS results showed higher Pd content compared with others.

Table 1. Pd content in samples determined by Vegard's law using XRD results, quantitative analysis by XPS, mass measurement and elemental mapping by STEM-EDS. Samples denoted as Cu50Pd10 refers to sputtering current was 50 mA for Cu target and 10 mA for Pd target, respectively.

	Pd content determined by different methods (at %)			
Sample	**XRD**	**XPS**	**Mass measurement**	**STEM-EDS**
Cu50Pd10	18	11	17	74 ± 2
Cu50Pd30	47	45	45	66 ± 3
Cu50Pd50	53	57	55	77 ± 3
Cu30Pd50	70	64	71	84 ± 5
Cu10Pd50	89	86	88	89 ± 2

Chapter 3 demonstrated the syntheses of Au@Cu_2O core-shell nanoparticles with a tunable Cu_2O shell thickness of 2-40 nm. The ethanol/water mixed solvent with high water content (>50 vol %) deteriorated the stability of the nanoparticles by oxidizing the Cu_2O shell to CuO in 5 days of storage. Although the Au@Cu_2O core-shell nanoparticles can initially provide metal/semiconductor interface as a potential terahertz wave emitter, the degradation leads the loss of unique properties of Cu_2O.

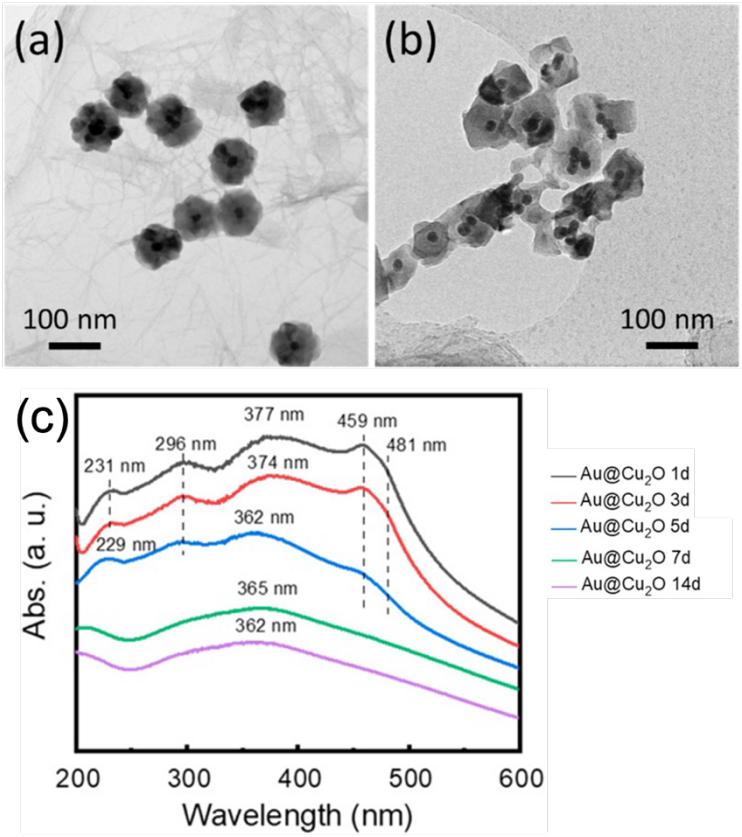

Figure 1. TEM images of (a) as-synthesized Au@Cu_2O core-shell nanoparticles and (b) after 5 days. (c) UV-vis absorption spectra of the Au@Cu_2O core-shell nanoparticles at different storage time. The nanoparticles were stored in an ethanol/water mixed solvent with composition of 30:70 in vol%.

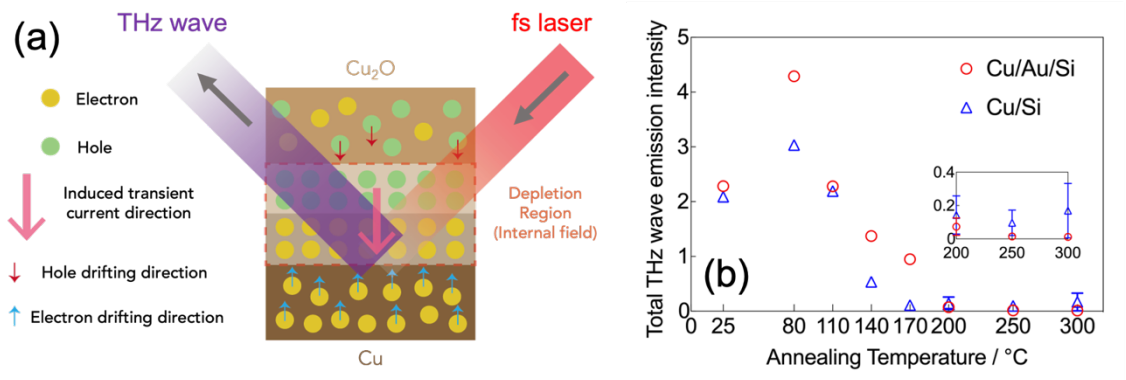

Figure 2. (a) Scheme and mechanism of terahertz wave emitted from Cu_2O/Cu interface under femtosecond laser irradiation. Mobility of holes is approximately one order lower than that of electrons. (b) Total terahertz wave emission intensity of annealed Cu/Si and Cu/Au/Si structures against different annealing conditions.

Chapter 4 showed the Cu_2O/Cu interface was the key factor of terahertz wave emission under femtosecond laser excitation. Cu_2O/Cu interface formed by annealing 80 nm thick Cu layer at a temperature of 80 to 140 °C can enhance the terahertz wave emission. It was because a depletion region was formed at Cu_2O/Cu interface. Charge carriers accelerated in the region when they were excited by the laser pulses, thus a transient current was induced as the terahertz wave source (Figure 2a). The terahertz wave emission was almost zero at an annealing temperature of ≥ 200 °C. It was because the Cu layer had transformed to Cu_2O and/or CuO that lack of Cu_2O/Cu interface. Terahertz wave emission intensities were stronger from double-layered Cu/Au structures (50 nm-thick Au layer) annealed at temperature ≤ 170 °C (Figure 2b). It was because the structures had greater light absorption for the Cu_2O/Cu interface, and underneath Au layer could reflect part of terahertz wave towards the detector.

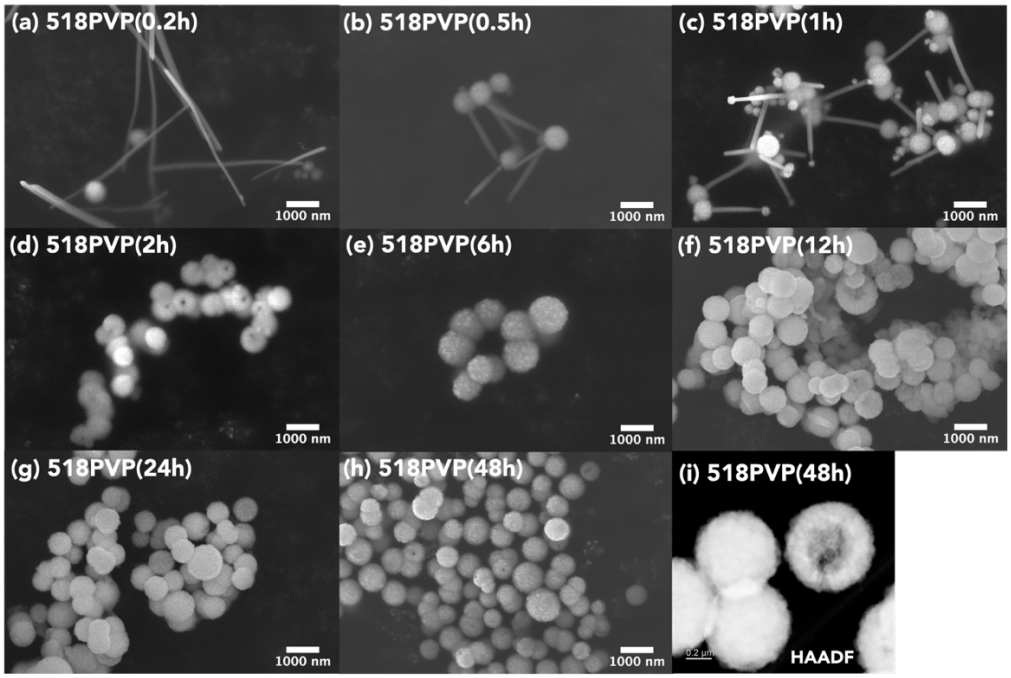

Figure 3. SEM images of product obtained with 518 mg of PVP at reaction time (a) 0.2 h, (b) 0.5 h, (c) 1 h, (d) 2 h, (e) 6 h, (f) 12 h, (g) 24 h, and (h) 48 h. (i) HAADF image of ZnTe microspheres shown in (h).

Chapter 5 demonstrated the sequential growth of 0.6 μm-sized ZnTe microspheres from 0.2 to 48 h. The size of microspheres were alternated with the amount of PVP used. At shorter reaction time, only Te rods were observed. Longer reaction time yielded more ZnTe microspheres (Figure 3a-h). Particularly, ZnTe microspheres nucleated and grew at the tip of Te rods when PVP was used because PVP adsorbed on the sides of Te rods to restrict nucleation and growth processes. ZnTe-Te interface was formed at the tip of Te rods for supplying Te^{2-} ions for the formation of ZnTe microspheres. Te rods were the sacrificial template for the growth of ZnTe microspheres (Figure 3b-d). A cavity was created in the center of ZnTe microspheres due to two reasons: (1) Te rods grew in a PVP-contained solution had a hollow-structured. There was no supply of Te^{2-} ions for the growth of center part of ZnTe microspheres. (2) Early formed ZnTe crystals had blocked the diffusion of Zn^{2+} ions towards the tip of Te rods. Thus, Te^{2-} ions diffused outwardly for the further growth of ZnTe crystals. These processes broke the ZnTe-Te interface during the growth of ZnTe microspheres and resulted in a cavity inside them (Figure 3i). ZnTe microspheres sized ≥ 1.6 μm loaded on Si wafer preliminarily showed terahertz wave emission under femtosecond laser excitation even though the ZnTe microspheres were polycrystalline.

[Conclusions]

Chapter 2 showed the detail characterizations and analyses of Cu-based nanoparticles formed by sputter deposition using different instruments. Sputter deposition had brought the ease of fabricating compositional-tunable alloy nanoparticles, yet challenges such as small amount of products and stability of products were remained for bringing the nanoparticles into practical use. Chapter 3 used wet-chemical method to

make heterostructure core-shell nanoparticles, which could not be obtained via sputter deposition. These two chapters had demonstrated using different approaches to synthesize desired structures in designing Cu-based nanomaterials.

Chapter 4 and 5 took a step forward to utilize nano/micro materials for terahertz wave emitting applications. Chapter 4 demonstrated the mechanism of terahertz wave irradiation from Cu_2O/Cu (semiconductor/metal) interface and emphasized the terahertz wave emission intensity enhancement with the use of Au layer under the Cu_2O/Cu interface. Chapter 5 focused on replacing the conventional single crystal of non-centrosymmetric materials with polycrystalline materials. In particular, polycrystalline ZnTe microspheres were used, with elucidating their sequential formation in a polyol system using a novel hot injection method. The preliminary results showed that polycrystalline ZnTe could emit terahertz wave.

Discussion in this dissertation has brought up to date knowledges on approaches to synthesize nano/micro materials and the optical response of these materials to the ultrafast laser pulses. The findings are further widening the availability of nano/micro materials for broadband terahertz pulse technologies.

[References]

1. Xu, J.; Zhao, T.; Liang, Z.; Zhu, L. Facile Preparation of AuPt Alloy Nanoparticles from Organometallic Complex Precursor. *Chem. Mater.*, **2008**, *20*(5), 1688-1690.
2. Okazaki, K.; Kiyama, T.; Hirahara, K.; Tanaka, N.; Kuwabata, S.; Torimoto, T. Single-step synthesis of gold-silver alloy nanoparticles in ionic liquids by a sputter deposition technique. *Chem. Commun.*, **2008**, 691-693.
3. Corpuz, R.D.; Ishida, Y.; Nguyen, M.T.; Yonezawa, T. Synthesis of positively

charged photoluminescent bimetallic Au–Ag nanoclusters by double-target sputtering method on a biocompatible polymer matrix. *Langmuir*, **2017**, *33*(36), 9144-9150.

4. Meischein, M.; Manjón, A.G.; Hammerschmidt, T.; Xiao, B.; Zhang, S.; Abdellaoui, L.; Scheu, C.; Ludwig, A. Elemental (im-)miscibility determines phase formation of multinary nanoparticles co-sputtered in ionic liquids. *Nanoscale Adv.*, **2022**, *4*, 3855-3869.
5. Wang, C.; Wang, C.; Xu, L.; Cheng, H.; Lin, Q.; Zhang, C. Protein-directed synthesis of pH-responsive red fluorescent copper nanoclusters and their applications in cellular imaging and catalysis. *Nanoscale*, **2014**, *6*, 1775-1781.
6. Chiba, M.; Nguyen M.T.; Hasegawa, Y.; Obora, Y.; Kwasaki, H.; Yonezawa, T. Synthesis of binary solid solution Cu–Pd nanoparticles by DMF reduction for enhanced photoluminescence properties. *J. Mater. Chem. C.*, **2015**, *3*, 514-520.
7. Chang, J.H.; Takai, T.; Godo, K.; Song, J.S.; Koo, B.H.; Hanada, T.; Yao, T. ZnTe-Based Light-Emitting-Diodes Grown on ZnTe Substrates by Molecular Beam Epitaxy. *Phys. Stat. Sol. (B)*, **2002**, *229*(2), 995-999.
8. Bang, J.; Park, J.; Lee, J.H.; Won, N.; Nam, J.; Lim, J.; Chang, B.Y.; Lee, H.J.; Chon, B.; Shin, J.; Park, J.B.; Choi, J.H.; Cho, K.; Park, S.M.; Joo, T.; Kim, S. ZnTe/ZnSe (Core/Shell) Type-II Quantum Dots: Their Optical and Photovoltaic Properties. *Chem. Mater.*, **2010**, *22*(1), 233-240.
9. Ferguson, B.; Zhang, X.-C. Materials for terahertz science and technology. *Nature Materials*, **2002**, *1*, 26-33.
10. Davies, A.G.; Linfield, E.H.; Johnston, M.B. The development of terahertz sources and their applications. *Phys. Med. Biol.*, **2002**, *47*, 3679.

11. Lu, X.; Yonezawa, T. Terahertz emission from Cu_xO/Au thin film. 2014 *MWP/APMP* **2014**, 164-165.
12. Lu, X.; Ishida, Y.; Mishina, T.; Nguyen, M. T.; Yonezawa, T. Enhanced Terahertz Emission from Cu_xO/Metal Thin Film Deposited on Columnar-Structured Porous Silicon. *Bull. Chem. Soc. Jpn.* **2015**, *88*, 10, 1385-1387.
13. Ramanandan, G. K. P.; Adam, A. J. L.; Ramakrishnan, G.; Petrik, P.; Hendrikx, R.; Planken, P. C. M. Optical characterization of gold-cuprous oxide interfaces for terahertz emission applications. *Appl. Opt.* **2014**, *53*, 10, 1994-2000.
14. Ramakrishnan, G.; Ramanandan, G. K. P.; Adam, A. J. L.; Xu, M.; Kumar, N.; Hendrikx, R. W. A.; Planken, P. C. M. Enhanced terahertz emission by coherent optical absorption in ultrathin semiconductor films on metals. *Opt. Express* **2013**, *21*, 14, 16784-16798.
15. Rice, A.; Jin, Y.; Ma, X.F.; Zhang, X.-C. Terahertz optical rectification from 〈110〉 zinc-blende crystals. *Appl. Phys. Lett.*, **1994**, *64*(11), 1324.
16. Zhang, X.-C.; Jin, Y.; Yang, K.; Schowalter, L.J. Resonant nonlinear susceptibility near the GaAs band gap. *Phys. Rev. Lett.*, **1992**, *69*, 2303.